Journal Pre-proof

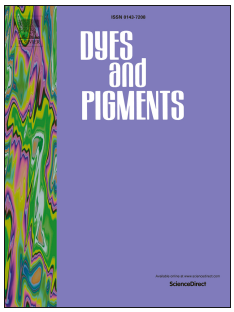

Bright near-infrared chemiluminescent dyes: Phthalhydrazides conjugated with fluorescent BODIPYs

Guanglei Li, Takashi Hirano, Koji Yamada

PII: S0143-7208(20)30319-3

DOI: https://doi.org/10.1016/j.dyepig.2020.108339

Reference: DYPI 108339

To appear in: *Dyes and Pigments*

Received Date: 5 February 2020

Revised Date: 5 March 2020

Accepted Date: 6 March 2020

Please cite this article as: Li G, Hirano T, Yamada K, Bright near-infrared chemiluminescent dyes: Phthalhydrazides conjugated with fluorescent BODIPYs, *Dyes and Pigments* (2020), doi: https://doi.org/10.1016/j.dyepig.2020.108339.

Guanglei Li: Methodology, Formal analysis, Investigation, Writing - Original Draft.
Takashi Hirano: Methodology, Formal analysis, Investigation, Resources, Writing - Review & Editing, Funding acquisition
Koji Yamada: Conceptualization, Methodology, Resources, Funding acquisition

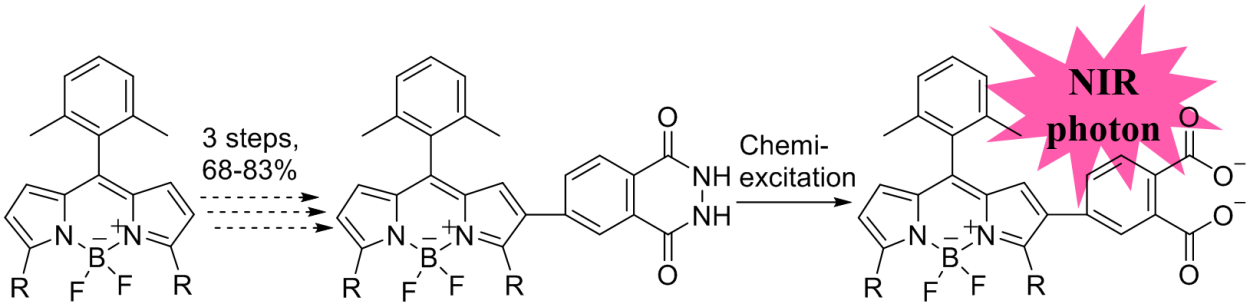

NIR fluorescence to NIR chemiluminescence

Bright Near-Infrared Chemiluminescent Dyes: Phthalhydrazides Conjugated with Fluorescent BODIPYs

Guanglei Li† Takashi Hirano,‡ and Koji Yamada*†

† Division of Materials Science, Graduate School of Environmental Science, Hokkaido University, Sapporo, Hokkaido 0860-0810, Japan

‡ Department of Engineering Science, Graduate School of Informatics and Engineering, The University of Electro-Communications, Chofu, Tokyo 182-8585, Japan

* Corresponding author, E-mail: yamada@ees.hokudai.ac.jp

ABSTRACT: A series of phthalhydrazides conjugated with NIR fluorescent BODIPY dyes were synthesized (three steps, overall yields 68–83%) and found to show strong NIR chemiluminescence (CL) with maxima in the range of 670–736 nm. One of these showed a CL quantum yield reaching 8.4 times higher than that of luminol. Tuning of the fluorescence band of the BODIPY unit directly leads to a red-shifted CL, developing a strategy for designing NIR chemiluminogens.

Keywords： Near-infrared, Chemiluminescent dyes, Phthalhydrazide, BODIPY

INTRODUCTION

Chemiluminescence (CL) is a phenomenon whereby photons are generated through a chemical reaction of a chemiluminogen. Compared with fluorescence analysis using an excitation light source, CL analysis provides data with no background noise arising from autofluorescence in a biological sample or from scattering of excitation light. Because of the high sensitivity and high signal-to-noise ratio of CL

detection, CL has been widely utilized in various chemical and biological analyses.[1] Luminol (5-amino-2,3-dihydrophthalazine-1,4-dione) is a chemiluminescent compound whose anion generated by deprotonation can be easily oxygenated by an appropriate biological, chemical, or electronic reaction leading to blue light emission with emission maximum around 420–450 nm. Besides its readily obtained luminescence, luminol possesses many advantages compared with other bio/chemiluminogens, such as good stability, low cost, and safety. The CL of luminol is widely used in biological analysis and *in vitro* imaging as a well-established sensitive technology.[1b, 2] The blue CL of luminol, however, hinders its application to *in vivo* systems due to significant light attenuation by tissues.[3] Hence, increasing the emission wavelength to the near-infrared (NIR) region would facilitate the *in vivo* application of luminol. For this purpose, luminol has recently been used in *in vivo* imaging with intermolecular energy transfer.[4] In this system, luminol functioned as an energy donor to stimulate a NIR fluorescent dye through sequential dual Förster resonance energy transfer (FRET). Because an efficiency of an intermolecular energy transfer is determined by the factors for FRET including the distance between an energy donor and an energy acceptor, emission intensities of the intermolecular CL systems will be affected by the reaction conditions. To overcome the weaknesses of this intermolecular energy transfer system, development of bio/chemiluminogens that produce NIR light is urgently required. Although efforts have been made to prepare phthalhydrazide-based CL systems,[5] to the best of our knowledge, no NIR systems with phthalhydrazide have been reported. To prepare NIR phthalhydrazide-based CL systems with high CL quantum yields, it is important to select an appropriate NIR fluorophore unit to combine

with the phthalhydrazide unit. As regards the NIR fluorophores, there are many candidates to choose. Recently, we developed NIR fluorescent BODIPYs **2a–c**[6] (Figure 1).

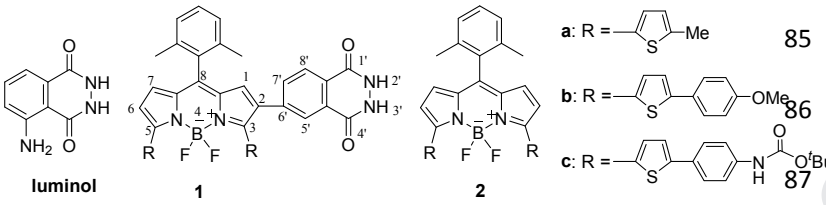

Figure 1. Structures of luminol, phthalhydrazide NIR BODIPY conjugates **1a–c**, and NIR BODIPYs **2a–c**.

The bulky 2,6-dimethylphenyl group at the C3 position in **2a–c** reduced aggregation and imparted good solubility and high fluorescence quantum yields. Phthalhydrazide NIR BODIPY conjugates **1a–c** were then designed by directly connecting the phthalhydrazide unit at the C6 position with the NIR BODIPY units at the C2 position. The direct connection of the phthalhydrazide and NIR BODIPY units is preferable to modulate the emission wavelength by intramolecular energy transfer, and the methodology of the direct connection will expand the derivatization range of the NIR CL compound. We report here the synthesis, spectroscopic properties, and CL properties of **1a–c.**

RESULTS AND DISSCUSSION

Phthalhydrazide conjugates **1a–c** were synthesized from BODIPYs **2a–c** and commercially available 5-bromophthalic anhydride **7** as shown in Scheme 1.

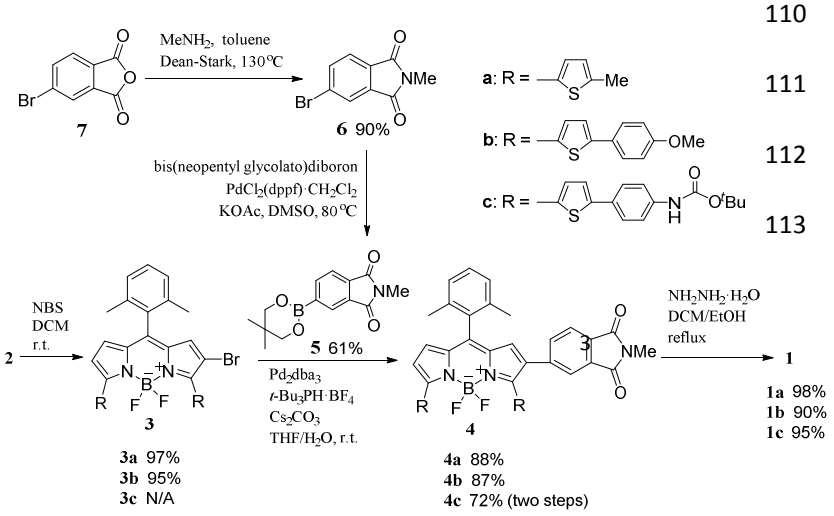

Scheme 1. Synthesis scheme of compounds **1a–c**

To synthesize the phthalhydrazide unit, *N*-methylphthalimide **6** was prepared from **7** with methylamine, and subsequent Miyaura–Ishiyama–Hartwig borylation of **6** yielded boronate **5**. BODIPYs **2a–c** were treated with one equivalent of NBS to afford monobromides **3a–c**, which were coupled with **5** to give phthalhydrazide precursors **4a–c**. Precursors **4a–c** readily reacted with excess hydrazine to afford **1a–c**. As we expected, **1a–c** showed good solubility in many organic solvents.

The spectroscopic properties of **1a–c** were investigated in acetone and DMSO (Figure 2), and the data are summarized in Table 1 together with those of **2a–c**[6] in dichloromethane (DCM) for comparison.

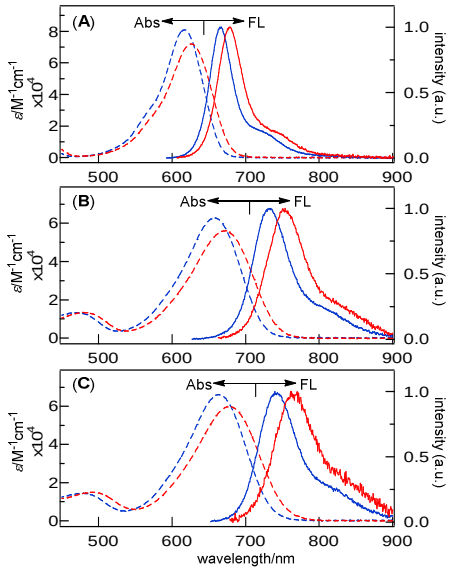

Figure 2. UV/vis absorption (Abs: dotted line) and fluorescence (FL: solid line) spectra of **1a** (A), **1b** (B), and **1c** (C) in acetone (blue) and DMSO (red).

Table 1. Spectroscopic data for **1a–c** in acetone and DMSO together with those for **2a–c** in DCM.

dye	solvent	λ_{abs} [a] /nm	ε [b] /M^{-1} cm^{-1}	λ_{fl} [c] /nm	Φ_{fl} [d]	Stokes shift/cm^{-1}
1a	acetone	617	81,000	667	0.85	1220
	DMSO	626	72,000	679	0.39	1250
2a[e]	DCM	640	66,000	662	0.81	520
1b	acetone	657	63,000	733	0.55	1580
	DMSO	670	56,000	754	0.27	1660
2b[e]	DCM	689	78,000	725	0.68	720
1c	acetone	662	66,000	740	0.31	1590
	DMSO	678	60,000	761	0.09	1610
2c[e]	DCM	691	82,000	740	0.53	960

[a] Absorption maximum. [b] Molar absorption coefficient. [c] Fluorescence emission maximum. [d] Absolute fluorescence quantum yield. [e] From reference **6**.

The absorption and emission bands of **1a**–**c** spanned a wide range of over the red and NIR regions. The absorption maxima (λ_{abs}) of the lowest energy bands of **1a**–**c** were observed in the range of 617–678 nm with large molar absorptivities (56,000–81,000 M^{-1} cm^{-1}), indicating that these absorption bands could be attributed to π–π* transitions. Fluorescence emission maxima (λ_{fl}) were in the 667–761 nm range with moderate Stokes shifts. As the solvent polarity increased from acetone (E_T^N 0.335) to DMSO (E_T^N 0.444),[7] both the λ_{abs} and λ_{fl} values were red-shifted by 9–16 nm and 12–21 nm, respectively. The Stokes shifts of **1a**–**c** in DMSO are slightly larger than those in acetone, indicating that the dipole moments of the excited singlet (S_1) states of **1a**–**c** were a little larger than those of the ground states. As the result, the S_1 states of **1a**–**c** were more stabilized by the more polar solvent (DMSO).[7] Therefore, the electronic excitations of **1a**–**c** have weak intramolecular charge-transfer character. The fluorescence quantum yields (Φ_{fl}) of **1a**–**c** in DMSO were about 1/3–1/2 lower than those in acetone. The polarization properties of the S_1 states of **1a**–**c** are known to influence the rate of non-radiative decay from the S_1 state in a polar solvent, resulting in lower Φ_{fl} values.[8] This result was consistent with previous reports on BODIPY systems.[9] It is noteworthy that the λ_{abs} values of **1a**–**c** were blue-shifted compared with those of **2a**–**c**, but the λ_{fl} values of **2a**–**c** were similar to those of **1a**–**c** in acetone. The result indicates that the phthalhydrazide units in **1a**–**c** showed π-conjugation with the BODIPY unit in the ground states, while the π-conjugation of the BODIPY and phthalhydrazide units was attenuated in the S_1 states of **1a**–**c**. Thus, the fluorescence emission properties of **1a**–**c** are mainly determined by the BODIPY unit. To rationalize the spectroscopic properties of **1a**–**c** and **2a**–**c**, DFT and TD-DFT calculations were performed for them using the B3LYP/6-31G(d) method (Figure 3, Table 2).[9a, 10]

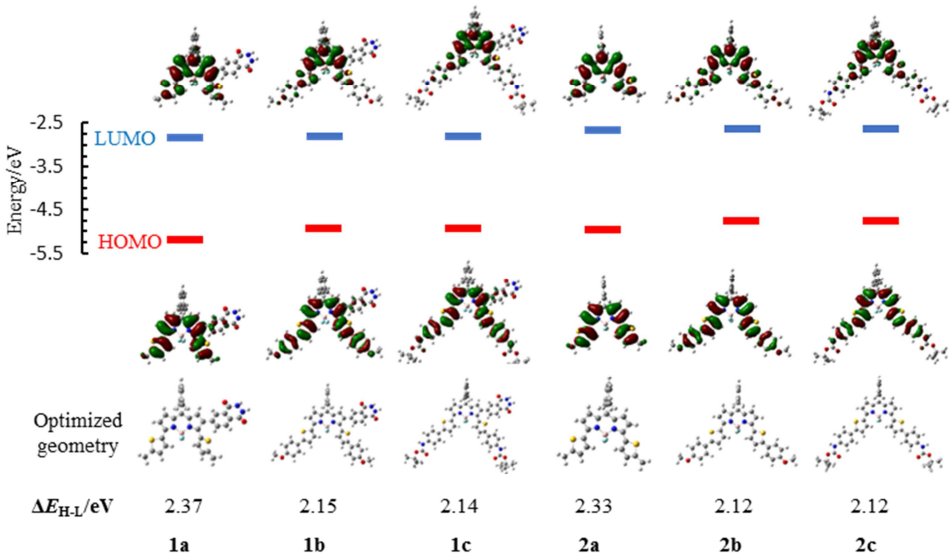

Figure 3. Frontier orbitals and optimized molecular structures of dyes **1a–c** and **2a–c**. The energy levels of the molecular orbital are denoted by blue and red bars. $\Delta E_{H\text{-}L}$ denotes the energy gap between HOMO and LUMO.

Table 2. Calculation data for **1** and **2** with DFT and TD-DFT using B3LYP/6-31G(d).

dye	HOMO /eV	LUMO /eV	ΔE_{H-L} [a] /eV	Transition [b]	λ_{tr} [c] /nm (*f*)	Configuration [d,e]
1a	−5.20	−2.82	2.37	$S_0 \rightarrow S_1$	546 (0.76)	H → L (99.5%) H ← L (2.2%)
1b	−4.95	−2.80	2.15	$S_0 \rightarrow S_1$	626 (0.92)	H → L (98.7%)
1c	−4.94	−2.80	2.14	$S_0 \rightarrow S_1$	633 (0.97)	H → L (98.5%)
2a	−4.98	−2.65	2.33	$S_0 \rightarrow S_1$	541 (0.69)	H → L (101.3%) H ← L (2.9%)
2b	−4.76	−2.64	2.12	$S_0 \rightarrow S_1$	616 (1.03)	H → L (100.2%) H ← L (2.1%)

2c	−4.76	−2.64	2.12	$S_0 \rightarrow S_1$	624 (1.10)	H → L (99.8%)

[a] Energy difference between HOMO and LUMO. [b] The π,π* transition to the excited singlet state with the lowest excitation energy. [c] Wavelengths estimated from transition energies. [d] Configuration of excitation. [e] H and L denote the HOMO and LUMO, respectively.

The optimized geometries of **1a**–**c** had dihedral angles between the phthalhydrazide and BODIPY units of 45.2° for **1a**, 46.3° for **1b**, and 45.1° for **1c**. The relatively non-planar molecular structures of **1a**–**c** may hinder aggregation of the dyes and also maintain communication between the phthalhydrazide units and BODIPY frameworks. The HOMO and LUMO levels of **1a**–**c** were lower than those of the corresponding BODIPY **2a**–**c** compounds, suggesting that the phthalhydrazide units behaved as electron-withdrawing groups in **1a**–**c**. The HOMO levels of **1b** and **1c** were higher than that of **1a** as with the series of **2**, indicating that the 4-methoxyphenyl and 4-BOC-aminophenyl groups in the BODIPY units effectively functioned as electron-donating π-conjugated substituents. Introducing the 4-methoxyphenyl and 4-BOC-aminophenyl groups to the BODIPY units increased the HOMO levels more effectively than the LUMO levels, leading to smaller HOMO–LUMO gaps (ΔE_{H-L}) for **1b** and **1c** compared with that of **1a**. The slightly blue-shifted λ_{abs} values of **1a**–**c** compared with those of **2a**–**c** were supported by the ΔE_{H-L} values. The ΔE_{H-L} values of **1a**–**c** were larger than those of **2a**–**c**, while the calculated wavelengths (λ_{tr}) estimated from the transition energies showed the opposite trend. Configuration interactions in the calculations would decrease the transition energies of **1a**–**c**. Interestingly, the LUMOs of **1a**–**c** had electron distributions only at the BODIPY frameworks, while their HOMOs had small electron distributions at the phthalhydrazide units.

The CL properties of **1a**–**c** and luminol were

evaluated with horseradish peroxidase (HRP) and H_2O_2 in MeOH/K_2CO_3 aqueous solutions. Figure 4 shows normalized CL spectra of **1a**–**c** together with that of luminol.

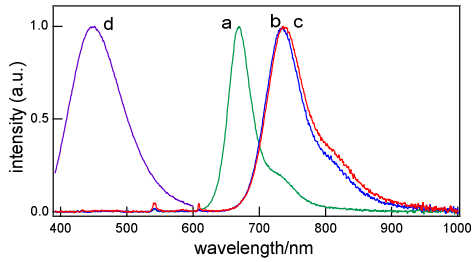

Figure 4. Normalized CL spectra of **1a** (a), **1b** (b), **1c** (c), and luminol (d).

Phthalhydrazide conjugates **1a**–**c** showed single sharp emission bands in the NIR region with maxima (λ_{CL}) in the 670–738 nm range, and no CL derived from the isolated phthalhydrazide units was observed. The λ_{CL} values of **1a**–**c** were similar to the λ_{fl} values of the corresponding BODIPY **2a**–**c** compounds, indicating that the BODIPY moieties in **1a**–**c** functioned effectively as fluorophore units. The CL reactions of **1a**–**c** gave the phthalate products oxy-**1a**–**c** in the S_1 states, and the excited state energies were used to generate the S_1 states of the BODIPY units.

The time courses of the CL reactions of **1a**–**c** traced by monitoring emission intensities showed that the emission intensities maximized immediately after mixing the reagents and gradually decreased (Figure S1). The half-lives of the emission intensities ($\tau_{1/2}$) are summarized in Table 3.

Table 3. Chemiluminescent parameters obtained for dyes **1a–c** and luminol.

dye	λ_{CL}/nm[a]	$\tau_{1/2}$/s[b]	rel. Φ_{CL}[c]

1a	670	145	8.4
1b	735	42	0.8
1c	736	22	0.4
luminol	451	6	1

[a] CL emission maximum. [b] Half-life of light emission. [c] Relative CL quantum yield.

The $\tau_{1/2}$ values follow the order **1a** > **1b** > **1c**, suggesting that the 4-methoxyphenyl and 4-BOC-aminophenyl groups in the BODIPY units accelerated the CL reactions as electron-donating substituents. The relative CL quantum yields (rel. Φ_{CL}) of **1a**–**c** were estimated using luminol as a standard.[11] It is noteworthy that **1a** showed higher CL efficiency (8.4-fold that of luminol), while **1b** and **1c** showed lower efficiencies (0.8-fold for **1b** and 0.4-fold for **1c**). In the CL reactions of **1a**–**c**, the S_1 states of the phthalate units in oxy-**1a**–**c** (Figure 5) were initially generated by the reactions of the anions of the phthalhydrazide units with superoxide anions.[12]

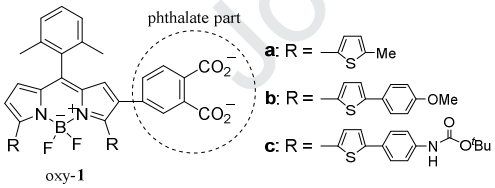

Figure 5. Phthalate products oxy-**1a**–**c** of CL reactions of **1a**–**c**.

The phthalate and BODIPY units in oxy-**1a**–**c** are connected by the single bond, leading to make a twisted but partially conjugated energy donor and acceptor system. Because the two units in oxy-**1a**–**c** are close to each other, the energy transfer process between the phthalate and BODIPY units will not be hindered by the need of spectral overlap for FRET as in the case of the through-bond energy transfer

cassettes.[13] Because of the partially π-electronic conjugation between the phthalate and BODIPY units, it may be better to understand that the CL reactions of **1a**–**c** directly generate the S_1 states of the whole molecules of oxy-**1a**–**c**. Characterization of the energy transfer processes in conjugated CL systems remained challenging.[5c]

CONCLUSIONS

In summary, we have developed the phthalhydrazide derivatives **1a**–**c**, which show NIR CL with HRP-H_2O_2. The NIR chemiluminogens were obtained by directly introducing NIR fluorescent BODIPYs into the phthalhydrazide skeleton at the C2 position. Their CL properties indicated that the direct conjugation strategy was suitable for providing a superior CL performance. Particularly, the observed CL maximum data indicated that various NIR chemiluminescent dyes could be developed by simply exchanging the BODIPY unit for one with a desired emission wavelength. Unfortunately, however, **1a**–**c** are insoluble in a 100% aqueous solution. Thus, it is necessary for *in vivo* applications to give further modification of the dye structure such as introducing a hydrophilic group. We believe that our present study provides a strategy for designing and preparing BODIPY-based NIR CL dyes, which can potentially be utilized for chemical and biological applications.

EXPERIMENTAL SECTION

General experimental. All commercially available solvents and reagents were used as received unless otherwise noted. Reactions were monitored with a silica gel TLC. Purification was performed on a silica gel chromatography. Melting points were determined with a Yamato MP-21 apparatus. ^{1}H and ^{13}C NMR spectra were recorded on a JEOL 400 spectrometer (400 MHz for ^{1}H NMR, 100 MHz for ^{13}C NMR) at

room temperature. Chemical shifts were expressed in parts per million (ppm) relative to TMS (0 ppm). Coupling constants (*J*) were expressed in Hz. HRMS were obtained on a Thermo Scientific Exactive under ESI or ACPI conditions. FT-IR spectra were recorded on a Thermo Nicolet iS10 spectrometer. UV/vis absorption spectra were measured with an Agilent Technologies Cary 60 spectrophotometer. Fluorescence spectra and fluorescence quantum yields were measured with Hamamatsu Photonics Quantaurus-QY Absolute PL quantum yield spectrometer C11347. CL spectra were recorded using an ATTO AB-1850 spectrophotometer or a PMA-12 Photonic multichannel analyzer C10027-02. CL kinetics were measured with an ATTO Luminescencer-Octa AB-2270. DFT calculations using the B3LYP functional with the 6-31G(d) basis set were performed on Gaussian 09 program, and the results were visualized in GaussView 5.

Chemiluminescence measurements. The relative CL quantum yields of the **1a–1c** were relatively determined by using that of luminol. Emission spectra of the **1a–1c** and luminol were measured with an AB-1850 spectrophotometer for detecting light intensity from the reaction mixture until the intensity of light decreased to the background level. For the measurements, a small portion of 500 μL stock solution of **1a–1c** (80 μM) or luminol (7 μM) in MeOH was added in a quartz cuvette placed in the spectrophotometer and was mixed with H_2O_2 (0.12 M in H_2O, 17 μL). The CL reaction was initiated by injecting HRP solution (10 μM in 0.1 M K_2CO_3, 500 μL) into the reaction mixture. All the measurements were conducted at room temperature (22 to 25 °C). Areas of the CL spectra obtained by integration per number of molecules of the **1a–1c** were calculated, and the ratios of the area values for **1a–1c** to that for luminol gave the relative CL quantum yields. As the CL bands of **1a–1c** exceeded the limitation of the AB-1850 spectrophotometer (400–800 nm), in order to show the whole spectra of **1a–1c**, the CL spectra were recorded with a PMA-12 photonic multichannel analyzer following the similar procedure.

Synthesis of 2-bromo-8-(2,6-dimethylphenyl)-3,5-bis(5-methylthien-2-yl)-4,4'-difluoro-4-bora-3a,4a-diaza-s-indacene (3a). To the solution of the starting **2a** (118 mg, 0.24 mmol) in DCM (5 mL) in an ice bath was added NBS (43 mg, 0.24 mmol) slowly. The reaction mixture was stirred at room temperature for 3 h. The reaction was quenched by adding an ice-cold saturated $NaHCO_3$ aqueous solution, and the products were extracted with DCM. The organic layers were combined, washed with H_2O and brine successively, and dried over Na_2SO_4. The solvent was evaporated under reduced pressure. The crude sample was purified by silica gel column chromatography using eluent gradients with the eluent pair hexane/ ethyl acetate (EA), to give **3a** as a dark red solid (133 mg, 97%). mp 189−191 °C. ^{1}H NMR (400 MHz, $CDCl_3$): δ (ppm) = 8.03 (d, *J* = 3.9 Hz, 1H), 7.65 (d, *J* = 4.0 Hz, 1H), 7.30−7.24 (m, 1H), 7.14 (d, *J* = 7.6 Hz, 2H), 6.87−6.84 (m, 2H), 6.74 (d, *J* = 4.3 Hz, 1H), 6.60 (d, *J* = 4.6 Hz, 1H), 6.52 (S, 1H), 2.58 (s, 3H), 2.53 (s, 3H), 2.19 (s, 6H). ^{13}C NMR (100 MHz, $CDCl_3$) δ: 167.74, 153.4, 147.1, 145.3, 144.3, 139.1, 137.5, 137.0, 133.6 (t, $J_{C\text{-}F}$ = 7.4 Hz), 132.7, 132.6 (t, $J_{C\text{-}F}$ = 4.8 Hz), 131.2, 130.7, 129.0, 128.4, 128.3, 127.4, 127.3, 125.8, 122.1, 20.2, 15.7, 15.5. FT-IR (ATR) *v*/cm^{-1}: 2915, 2847, 1558, 1538, 1486, 1462, 1438, 1403, 1375. HRMS (ESI, Orbitrap) m/z: $[M+Na]^+$ Calcd for $C_{27}H_{22}N_2{}^{10}BBrF_2NaS_2$ 588.0401, Found 588.0402.

Synthesis of 2-bromo-8-(2,6-dimethylphenyl)-3,5-bis[5-(4-methoxyphenyl)thien-2-yl]-4,4'-difluoro-4-bora-3a,4a-diaza-s-indacene (3b). A preparation according to the procedure similar to **3a** by using **2b** (150 mg, 0.22 mmol), NBS (40 mg, 0.22 mmol) and DCM (4 mL) afforded **3b**as a black solid (157 mg, 95%). mp 230−231 °C. ^{1}H NMR (400 MHz, $CDCl_3$): δ (ppm) = 8.24 (d, *J* = 4.1 Hz, 1H), 7.88 (d, *J* = 4.3 Hz, 1H), 7.64 (d, *J* = 8.7 Hz, 2H), 7.58 (d, *J* = 8.8 Hz, 2H), 7.33−7.27 (m, 3H), 7.15 (d, *J* = 7.6 Hz, 2H), 6.95-

6.91 (m, 4H), 6.84 (d, J = 4.4 Hz, 1H), 6.62 (d, J = 4.5 Hz, 1H), 6.56 (s, 1H), 3.85 (s, 3H), 3.83 (s, 3H), 2.22 (s, 6H). ^{13}C NMR (100 MHz, $CDCl_3$) δ: 160.2, 159.6, 152.8, 150.2, 148.2, 145.0, 138.6, 137.8, 137.1, 134.4 (t, J_{C-F} = 8.2 Hz), 134.0, 133.6 (t, J_{C-F} = 5.6 Hz), 132.7, 131.6, 130.6, 129.2, 129.0, 127.5, 127.46, 127.42, 126.2, 124.8, 122.5, 122.3, 114.5, 114.3, 107.9, 55.41, 55.36, 20.2. FT-IR (ATR) ν/cm^{-1}: 2988, 2901, 1603, 1559, 1536, 1510, 1479, 1449, 1430. HRMS (ESI, Orbitrap) m/z: $[M+Na]^+$ Calcd for $C_{39}H_{30}O_2N_2{}^{10}BBrF_2NaS_2$ 772.0922, Found 772.0931.

Synthesis of 8-(2,6-dimethylphenyl)-2-(2-methyl-1,3-dioxoisoindolin-5-yl)-3,5-bis(5-methylthien-2-yl)-4,4'-difluoro-4-bora-3a,4a-diaza-s-indacene (4a). Compounds **3a** (96 mg, 0.17 mmol), **5** (70 mg, 0.26 mmol), tris(dibenzylideneacetone)dipalladium (0) (Pd_2dba_3) (16 mg, 0.017 mmol), tri-*tert*-butylphosphonium tetrafluoroborate ([(*t*-Bu)$_3$PH]BF_4) (10 mg, 0.034 mmol) and Cs_2CO_3 (222 mg, 0.68 mmol) were placed in a two-necked round bottom flask. Prior to the addition of THF/H_2O (3 mL/20 μL), the flask was purged with N_2 three times. The reaction mixture was stirred at 25 °C for 24 h, then the product was extracted with DCM. The organic layers were combined, washed with H_2O and brine successively, and dried over Na_2SO_4. The solvent was evaporated under reduced pressure. The crude sample was purified by silica gel column chromatography using eluent gradients with the eluent pair hexane/DCM, to give **4a** as a dark red solid (96 mg, 88%). mp 288−289 °C. ^{1}H NMR (400 MHz, $CDCl_3$): δ (ppm) = 8.06 (d, J = 3.8 Hz, 1H), 7.65−7.63 (m, 2H), 7.39 (dd, J = 7.6 Hz, J = 1.6 Hz, 1H), 7.33−7.29 (m, 2H), 7.17 (d, J = 7.8 Hz, 2H), 6.87 (d, J = 3.9 Hz, 1H), 6.79 (d, J = 4.1 Hz, 2H), 6.65 (d, J = 4.6 Hz, 1H), 6.57 (s, 1H), 3.14 (s, 3H), 2.55 (s, 3H), 2.50 (s, 3H), 2.25 (s, 6H). ^{13}C NMR (100 MHz, $CDCl_3$): 168.4, 168.3, 153.6, 147.2, 144.9, 144.1, 141.1, 139.9, 137.9, 137.0, 134.1, 133.8 (t, J_{C-F} = 7.4 Hz), 133.7, 132.9, 132.4, 131.9 (t, J_{C-F} = 3.2 Hz), 131.6, 131.1, 130.8, 129.8, 129.2, 129.0, 128.3, 127.5, 126.0, 124.5, 123.0,

122.9, 122.3, 23.9, 20.2, 15.7, 15.5. FT-IR (ATR) ν/cm^{-1}: 2913, 1768, 1708, 1558, 1537, 1481, 1463, 1422, 1374. HRMS (ESI, Orbitrap) m/z: $[M+Na]^+$ Calcd for $C_{36}H_{28}O_2N_3{}^{10}BF_2NaS_2$ 669.1622, Found 669.1622.

Synthesis of 8-(2,6-dimethylphenyl)-2-(2-methyl-1,3-dioxoisoindolin-5-yl)-3,5-bis[5-(4-methoxyphenyl)thien-2-yl]-4,4'-difluoro-4-bora-3a,4a-diaza-s-indacene (4b). A preparation according to the procedure similar to **2a** by using **3b** (120 mg, 0.16 mmol), 5 (65 mg, 0.24 mmol), Pd_2dba_3 (15 mg, 0.016 mmol), $[(t\text{-}Bu)_3PH]BF_4$ (9 mg, 0.03 mmol), Cs_2CO_3 (209 mg, 0.64 mmol) and THF/H_2O (3 mL/20 μL) afforded 4b as a dark green solid (115 mg, 87%). mp 155−157 °C. ^{1}H NMR (400 MHz, $CDCl_3$): δ (ppm) = 8.26 (d, J = 4.0 Hz, 1H), 7.70 (s, 1H), 7.63 (d, J = 7.8 Hz, 1H), 7.56-7.54 (m, 3H), 7.50 (d, J = 8.8 Hz, 2H), 7.45 (d, J = 8.6 Hz, 1H), 7.32−7.27 (m, 2H), 7.25−7.24 (m, 1H), 7.17 (d, J = 7.6 Hz, 2H), 6.90−6.86 (m, 5H), 6.67 (d, J = 4.6 Hz, 1H), 6.61 (s, 1H), 3.79 (s, 6H), 3.12 (s, 3H), 2.26 (s, 6H). ^{13}C NMR (100 MHz, $CDCl_3$) δ: 168.3, 168.2, 160.1, 159.5, 153.1, 150.4, 148,0, 144.4, 140.9, 139.5, 138.2, 137.0, 134.6 (t, $J_{C\text{-}F}$ = 7.8 Hz), 134.4, 133.8, 132.9 (t, $J_{C\text{-}F}$ = 3.5 Hz), 132.8, 132.4, 131.9, 131.4, 130.8, 130.0, 129.8, 129.0, 127.5, 127.4, 127.2, 126.6, 126.0, 124.8, 124.7, 123.0, 122.9, 122.6, 122.5, 114.40, 114.2, 55.3, 23.9, 20.2. FT-IR (ATR) ν/cm^{-1}: 2988, 2901, 1770, 1711, 1605, 1536, 1510, 1476, 1488, 1431. HRMS (ESI, Orbitrap) m/z: $[M+Na]^+$ Calcd for $C_{48}H_{36}O_4N_3{}^{10}BF_2NaS_2$ 853.2137, Found 853.2155.

Synthesis of 8-(2,6-dimethylphenyl)-2-(2-methyl-1,3-dioxoisoindolin-5-yl)-3,5-bis{5-[4-((*N*-*tert*-butoxycarbonyl)amino)phenyl]thien-2-yl}-4,4'-difluoro-4-bora-3a,4a-diaza-s-indacene (4c). The starting compound **3c** was prepared according to the procedure similar to **3a** by using **2c** (60 mg, 0.07 mmol), NBS (13 mg, 0.07 mmol) and DCM (2 mL). The crude compound **3c** was used for the next reaction without

purification. A preparation according to the procedure similar to **2a** by using the crude **3c**, **5** (29 mg, 0.1 mmol), Pd_2dba_3 (6 mg, 0.007 mmol), $[(t\text{-}Bu)_3PH]BF_4$ (4 mg, 0.014 mmol), Cs_2CO_3 (91 mg, 0.28 mmol) and THF/H_2O (1.5 mL/10 μL) afforded **4c** as a dark red solid (51 mg, two step overall yield 72%). mp 185−187 °C. ^{1}H NMR (400 MHz, $CDCl_3$): δ (ppm) = 8.25 (d, *J* = 4.2 Hz, 1H), 7.70 (s, 1H), 7.65 (d, *J* = 7.8 Hz, 1H), 7.58 (d, *J* = 8.7 Hz, 2H), 7.53−7.49 (m, 3H), 7.45 (d, *J* = 7.8 Hz, 1H), 7.41 (d, *J* = 8.6 Hz, 2H), 7.37−7.30 (m, 4H), 7.28−7.26 (m, 1H), 7.19 (d, *J* = 7.7 Hz, 2H), 6.88 (d, *J* = 4.6 Hz, 1H), 6.69 (d, *J* = 4.6 Hz, 1H), 6.60 (s, 1H), 6.59 (bs, 1H), 6.54 (bs, 1H), 3.14 (s, 3H), 2.27 (s, 6H), 1.53 (s, 9H) , 1.52 (s, 9H). ^{13}C NMR (100 MHz, $CDCl_3$) δ: 168.4, 168.3, 153.1, 152.5, 152.4, 150.2, 147.9, 144.5, 141.0, 139.7, 139.0, 138.3, 137.1, 134.6 (t, $J_{C\text{-}F}$ = 7.6 Hz), 134.5, 133.9, 133.0 (t, $J_{C\text{-}F}$ = 3.7 Hz), 132.8, 132.5, 131.8, 130.9, 130.2, 130.1, 129.1, 128.6, 128.1, 127.6, 126.9, 126.6, 125.1, 124.8, 123.1, 123.0, 122.6, 118.65, 118.59, 80.9, 80.7, 28.3, 24.0, 20.3. FT-IR (ATR) ν/cm^{-1}: 2973, 2901, 1771, 1711, 1607, 1538, 1478, 1435, 1409, 1378. HRMS (ESI, Orbitrap) m/z: $[M+Na]^+$ Calcd for $C_{56}H_{50}O_6N_5{}^{10}BF_2NaS_2$ 1023.3192, Found 1023.3212.

Synthesis of 8-(2,6-dimethylphenyl)-2-(1,4-dioxo-1,2,3,4-tetrahydrophthalazin-6-yl)-3,5-bis(5-methylthien-2-yl)-4,4'-difluoro-4-bora-3a,4a-diaza-s-indacene (1a). A solution of **4a** (65 mg, 0.10 mmol) and hydrazine monohydrate ($NH_2NH_2\cdot H_2O$, 50 μL, 1 mmol) in ethanol/DCM (3 mL/6 mL) was refluxed under N_2 for 24 h. After cooling to room temperature, the solvent was removed under reduced pressure. The residue was purified by silica gel column chromatography using eluent gradients with the eluent pair hexane/acetone to give **1a** as a dark purple solid (64 mg, 98%). mp 240−242 °C. ^{1}H NMR (400 MHz, $CDCl_3$): δ (ppm) = 13.55 (bs, 1H), 12.34 (bs, 1H), 8.14 (s, 1H), 8.07−8.03 (m, 2H), 7.53 (d, *J* = 8.2 Hz, 1H), 7.33−7.30 (m, 2H), 7.19 (d, *J* = 7.6 Hz, 2H), 6.87 (d, *J* = 3.4 Hz, 1H), 6.79−6.78 (m, 2H), 6.69 (s,

1H), 6.66 (d, J = 4.5Hz, 1H), 2.55 (s, 3H), 2.51 (s, 3H), 2.27 (s, 6H). ^{13}C NMR (100 MHz, $CDCl_3$) δ: 158.2, 157.5, 153.5, 147.1, 145.3, 144.2, 140.3, 140.1, 137.9, 137.0, 134.3, 133.74, 133.69 (t, J_{C-F} = 7.8 Hz), 132.9, 132.1 (t, J_{C-F} = 3.7 Hz), 131.8, 131.2, 130.8, 129.3, 129.0, 128.3, 127.6, 127.2, 126.1, 125.4, 125.1, 124.9, 122.2, 20.3, 15.7, 15.5. FT-IR (ATR) ν/cm^{-1}: 2988, 2901, 1661, 1559, 1543, 1489, 1462, 1408. HRMS (ESI, Orbitrap) m/z: $[M+Na]^+$ Calcd for $C_{35}H_{27}O_2N_4{}^{10}BF_2NaS_2$ 670.1565, Found 670.1574.

Synthesis of 8-(2,6-dimethylphenyl)-2-(1,4-dioxo-1,2,3,4-tetrahydrophthalazin-6-yl)-3,5-bis[5-(4-methoxyphenyl)thien-2-yl]-4,4'-difluoro-4-bora-3a,4a-diaza-s-indacene (1b). A preparation according to the procedure similar to **1a** by using **4b** (42 mg, 0.05 mmol), $NH_2NH_2{\cdot}H_2O$ (28 μL, 0.75 mmol), and ethanol/DCM (3 mL/3 mL) afforded **1b** as a dark purple solid (38 mg, 90%). mp 202−204 °C. ^{1}H NMR (400 MHz, $CDCl_3$): δ (ppm) = 13.60 (bs, 1H), 12.27 (bs, 1H), 8.28 (d, J = 4.2 Hz, 1H), 8.20 (s, 1H), 8.06 (d, J = 8.3 Hz, 1H), 7.62−7.59 (m, 3H), 7.54−7.51 (m, 3H), 7.33−7.31 (m, 2H), 7.26−7.25 (m, 1H), 7.20 (d, J = 7.7 Hz, 2H), 6.94 (d, J = 8.8 Hz, 2H), 6.90−6.87 (m, 3H), 6.71−7.69 (m, 2H), 3.85 (s, 3H), 3.81 (s, 3H), 2.29 (s, 6H). ^{13}C NMR (100 MHz, $CDCl_3$) δ: 160.2, 159.5, 158.3, 157.4, 152.9, 150.2, 148.2, 144.8, 140.2, 139.8, 138.2, 137.1, 134.6, 134.5 (t, J_{C-F} = 7.4 Hz), 133.9, 133.1 (t, J_{C-F} = 4.5 Hz), 132.9, 132.1, 131.6, 131.0, 130.8, 130.0, 129.1, 127.6, 127.5, 127.3, 126.7, 126.2, 125.4, 125.3, 125.0, 124.9, 122.7, 122.4, 114.5, 114.3, 55.4, 55.3, 20.3. FT-IR (ATR) ν/cm^{-1}: 2989, 2901, 1720, 1657, 1605, 1538, 1475, 1450, 1435, 1407. HRMS (ESI, Orbitrap) m/z: $[M+Na]^+$ Calcd for $C_{47}H_{35}O_4N_4{}^{10}BF_2NaS_2$ 854.2089, Found 854.2105.

Synthesis of 8-(2,6-dimethylphenyl)-2-(1,4-dioxo-1,2,3,4-tetrahydrophthalazin-6-yl)-3,5-bis{5-[4-((*N*-*tert*-butoxy

carbonyl)amino)phenyl]thien-2-yl}-4,4'-difluoro-4-bora-3a,4a-diaza-s-indacene (1c). A preparation according to the procedure similar to **1a** by using **4c** (30 mg, 0.015 mmol), $NH_2NH_2 \cdot H_2O$ (45 μL, 0.45 mmol), and ethanol/DCM (3 mL/3 mL) afforded **1c** as a dark purple solid (29 mg, 95%). mp > 300 °C. ^{1}H NMR (400 MHz, $CDCl_3$): δ (ppm) = 13.59 (bs, 1H), 12.28 (bs, 1H), 8.27 (d, *J* = 3.7 Hz, 1H), 8.19 (s, 1H), 8.06 (d, *J* = 8.2 Hz, 1H), 7.61−7.58 (m, 3H), 7.54 (d, *J* = 3.4 Hz, 1H), 7.50 (d, *J* = 7.9 Hz, 2H), 7.41 (d, *J* = 8.0 Hz, 2H), 7.35−7.32 (m, 4H), 7.28−7.26 (m,1H), 7.20 (d, *J* = 7.6 Hz, 2H), 6.88 (d, *J* = 4.1 Hz, 1H), 6.70−6.69 (m, 2H), 6.60 (s, 2H), 2.29 (s, 6H), 1.53 (s, 9H), 1.51 (s, 9H). ^{13}C NMR (100 MHz, $CDCl_3$) δ: 158.2, 157.4, 152.9, 152.6, 152.5, 149.9, 147.9, 144.9, 140.1, 139.9, 139.0, 138.3, 137.0, 134.7, 134.4, 133.9, 133.1, 132.8, 132.2, 131.9, 131.0, 130.8, 130.2, 129.1, 128.6, 128.1, 127.6, 126.8, 126.7, 125.5, 125.4, 125.1, 123.0, 122.4, 118.7, 118.6, 80.9, 80.6, 28.3, 20.3. FT-IR (ATR) ν/cm^{-1}: 2973, 2917, 1705, 1652, 1538, 1475, 1447, 1409, 1364. HRMS (ESI, Orbitrap) m/z: $[M+Na]^+$ Calcd for $C_{55}H_{49}O_6N_6{}^{10}BF_2NaS_2$ 1024.3145, Found 1024.3160.

Synthesis of 5-bromo-2-methylisoindoline-1,3-dione (6). 5-Bromophthalic anhydride **7** (1.14 g, 5.0 mmol), methylamine (0.65 mL of 40 wt% in H_2O, 7.5 mmol) and toluene (25 mL) were placed in a round bottom flask and purged with N_2 three times. The flask fitted with a Dean-Stark trap, and the mixture was refluxed for 12 h. After cooling to room temperature, the solvent was evaporated under reduced pressure. The residue was purified by silica gel column chromatography (EA: hexane 1: 9) to yield **6** as white solid (1.52 g, 90%). mp 145−146 °C. ^{1}H NMR (400 MHz, $CDCl_3$): δ (ppm) = 7.97 (d, *J* =1.0 Hz, 1H), 7.84 (dd, *J* =7.8 Hz, *J* =1.5 Hz, 1H), 7.70 (d, *J* = 7.9 Hz, 1H), 3.17 (s, 3H). ^{13}C NMR (100 MHz, $CDCl_3$) δ: 167.6, 167.0, 136.9, 133.8, 130.7, 128.8, 126.6, 124.6, 24.1. FT-IR (ATR) ν/cm^{-1}: 1762, 1707, 1601, 1432, 1415, 1380. HRMS (ESI, Orbitrap) m/z: $[M+H]^+$ Calcd for $C_9H_7O_2NBr$ 239.9655, Found 239.9660.

Synthesis of 5-(5,5-dimethyl-1,3,2-dioxaborinan-2-yl)-2-methylisoindole-1,3-dione (5). Compound **6** (1.51 g, 6.29 mmol), bis(neopentyl glycolato)diboron (1.42 g, 6.29 mmol), potassium acetate (KOAc) (1.85 g, 18.9 mmol) and $PdCl_2(dppf)\cdot CH_2Cl_2$ (154 mg, 0.19 mmol, 3 mol%) were placed in a two-necked round bottom flask. The flask was then purged with N_2 three times before addition of 16 mL of DMSO. The mixture was stirred at 80 ℃ for 22 h. After the reaction was complete, the mixture was extracted with EA, washed with H_2O and brine successively, and the organic layer was collected, dried over Na_2SO_4 and evaporated to dryness under reduced pressure. The residue was purified by silica gel column chromatography (EA: hexane 1: 9 to 1: 4) to yield 5 as white solid (1.04 g, 61%). mp 189−190 °C. ^{1}H NMR (400 MHz, $CDCl_3$): δ (ppm) = 8.27 (s, 1H), 8.13 (d, J = 0.7 Hz, 1H), 7.80 (d, J = 0.8 Hz, 1H), 3.80 (s, 4H), 3.18 (s, 3H), 1.04 (s, 6H). ^{13}C NMR (100 MHz, $CDCl_3$) δ: 168.8, 168.7, 139.5, 133.9, 131.2, 128.4, 122.1, 72.5, 31.9, 23.9, 21.8. FT-IR (ATR) ν/cm^{-1}: 2959, 2930, 1770, 1709, 1618, 1480, 1593, 1432, 1414, 1375. HRMS (ACPI, Orbitrap) m/z: $[M+H]^+$ Calcd for $C_{14}H_{17}O_4N^{10}B$ 273.1282, Found 273.1282.

Supplementary information

The supplement information is available.

CL kinetic profiles of **1a**–**1c** and luminol. ^{1}H and ^{13}C NMR spectra. DFT and TD-DFT calculation results for **1a-1c**, **2a-2c**.

ACKNOWLEDGEMENT

This work was partially supported by JSPS KAKENHI Grants (JP17H06371 and JP18K05075 for TH). We acknowledge Mr. Yasuhide Fukuyo for his help on synthesis experiments. We thank the Information Technology Center of UEC for technical assistance in computing DFT calculations. We thank Ms. Miho Yamada, the Instrument Analysis Division, Hokkaido University for measuring the mass spectra.

References

1. (a) Roda, A.; Guardigli, M., Analytical chemiluminescence and bioluminescence: latest achievements and new horizons. *Anal. Bioanal. Chem.* **2012,** *402*, 69-76; (b) Roda, A.; Pasini, P.; Guardigli, M.; Baraldini, M.; Musiani, M.; Mirasoli, M., Bio-and chemiluminescence in bioanalysis. *Fresenius J. Anal. Chem.* **2000,** *366*, 752-759.

2. Alshetaiwi, H. S.; Balivada, S.; Shrestha, T. B.; Pyle, M.; Basel, M. T.; Bossmann, S. H.; Troyer, D. L., Luminol-based bioluminescence imaging of mouse mammary tumors. *J. Photochem. Photobiol. B* **2013,** *127*, 223-228.

3. (a) Weissleder, R., A clearer vision for in vivo imaging. *Nat. Biotechnol.* **2001,** *19*, 316-317; (b) Lee, E. S.; Deepagan, V.; You, D. G.; Jeon, J.; Yi, G.-R.; Lee, J. Y.; Lee, D. S.; Suh, Y. D.; Park, J. H., Nanoparticles based on quantum dots and a luminol derivative: implications for in vivo imaging of hydrogen peroxide by chemiluminescence resonance energy transfer. *Chem. Commun.* **2016,** *52*, 4132-4135; (c) Tseng, J.-C.; Kung, A. L., In vivo imaging of inflammatory phagocytes. *Chem. Biol.* **2012,** *19*, 1199-1209; (d) Gross, S.; Gammon, S. T.; Moss, B. L.; Rauch, D.; Harding, J.; Heinecke, J. W.; Ratner, L.; Piwnica-Worms, D., Bioluminescence imaging of myeloperoxidase activity in vivo. *Nat. Med.* **2009,** *15*, 455.

4. Liu, R.; Tang, J.; Xu, Y.; Dai, Z., Bioluminescence Imaging of Inflammation in Vivo Based on Bioluminescence and Fluorescence Resonance Energy Transfer Using Nanobubble Ultrasound Contrast Agent. *ACS nano* **2019,** *13*, 5124-5132.

5. (a) Degirmenci, A.; Algi, F., Synthesis, chemiluminescence and energy transfer efficiency of 2, 3-dihydrophthalazine-1, 4-dione and BODIPY dyad. *Dyes Pigm.* **2017,** *140*, 92-99; (b) Bag, S.; Tseng, J.-C.; Rochford, J., A BODIPY-luminol chemiluminescent resonance energy-transfer (CRET) cassette for imaging

of cellular superoxide. *Org. Biomol. Chem.* **2015,** *13*, 1763-1767; (c) Han, J.; Jose, J.; Mei, E.; Burgess, K., Chemiluminescent Energy‐Transfer Cassettes Based on Fluorescein and Nile Red. *Angew. Chem. Int. Ed.* **2007,** *46*, 1684-1687.

6. Li, G.; Otsuka, Y.; Matsumiya, T.; Suzuki, T.; Li, J.; Takahashi, M.; Yamada, K., A Straightforward Substitution Strategy to Tune BODIPY Dyes Spanning the Near-Infrared Region via Suzuki–Miyaura Cross-Coupling. *Materials* **2018,** *11*, 1297.

7. Reichardt, C., Solvatochromic dyes as solvent polarity indicators. *Chem. Rev.* **1994,** *94*, 2319-2358.

8. Umezawa, K.; Matsui, A.; Nakamura, Y.; Citterio, D.; Suzuki, K., Bright, color-tunable fluorescent dyes in the Vis/NIR region: establishment of new "tailor-made" multicolor fluorophores based on borondipyrromethene. *Chem. Eur. J.* **2009,** *15*, 1096-1106.

9. (a) Xuan, S.; Zhao, N.; Ke, X.; Zhou, Z.; Fronczek, F. R.; Kadish, K. M.; Smith, K. M.; Vicente, M. G. H., Synthesis and spectroscopic investigation of a series of push–pull boron dipyrromethenes (BODIPYs). *J. Org. Chem.* **2017,** *82*, 2545-2557; (b) Shi, W.-J.; Lo, P.-C.; Singh, A.; Ledoux-Rak, I.; Ng, D. K., Synthesis and second-order nonlinear optical properties of push-pull BODIPY derivatives. *Tetrahedron* **2012,** *68*, 8712-8718; (c) Qin, W.; Baruah, M.; Van der Auweraer, M.; De Schryver, F. C.; Boens, N., Photophysical properties of borondipyrromethene analogues in solution. *J. Phys. Chem. A* **2005,** *109*, 7371-7384.

10. (a) Nano, A.; Ziessel, R.; Stachelek, P.; Harriman, A., Charge‐Recombination Fluorescence from Push–Pull Electronic Systems Constructed around Amino‐Substituted Styryl–BODIPY Dyes. *Chem. Eur. J.* **2013,** *19*, 13528-13537; (b) Jiao, C.; Huang, K.-W.; Wu, J., Perylene-fused BODIPY dye with near-IR absorption/emission and high photostability. *Org. Lett.* **2011,** *13*, 632-635.

11. Ando, Y.; Niwa, K.; Yamada, N.; Irie, T.; Enomoto, T.; Kubota, H.; Ohmiya, Y.; Akiyama, H., Development of a Quantitative Bio/Chemiluminescence Spectrometer Determining Quantum Yields: Re-

examination of the Aqueous Luminol Chemiluminescence Standard. *Photochem. Photobiol*. **2007,** *83*, 1205-1210.

12. Merényi, G.; Lind, J.; Eriksen, T. E., Luminol chemiluminescence: chemistry, excitation, emitter. *J. Biolumin. Chemilumin.* **1990,** *5*, 53-56.

13. (a) Wan, C. W.; Burghart, A.; Chen, J.; Bergström, F.; Johansson, L. B. Å.; Wolford, M. F.; Kim, T. G.; Topp, M. R.; Hochstrasser, R. M.; Burgess, K., Anthracene–BODIPY cassettes: syntheses and energy transfer. *Chem. Eur. J.* **2003,** *9*, 4430-4441; (b) Fan, J.; Hu, M.; Zhan, P.; Peng, X., Energy transfer cassettes based on organic fluorophores: construction and applications in ratiometric sensing. *Chem. Soc. Rev.* **2013,** *42*, 29-43.

Declaration of interests

☒ The authors declare that they have no known competing financial interests or personal relationships that could have appeared to influence the work reported in this paper.

☐The authors declare the following financial interests/personal relationships which may be considered as potential competing interests: